

# Field-induced spin mixing in ultrathin superconducting Al and Be films in high parallel magnetic fields

P.W. Adams

*Department of Physics and Astronomy  
Louisiana State University  
Baton Rouge, Louisiana, 70803*

(Dated: September 29, 2018)

We report spin-dependent electron density of states (DOS) studies of ultra-thin superconducting Al and Be films in high parallel magnetic fields. Superconductor-insulator-superconductor (SIS) tunneling spectra are presented in which both the film and the counterelectrode are in the paramagnetic limit. This SIS configuration is exquisitely sensitive to spin mixing and/or spin flip processes which are manifest as DOS singularities at  $eV = 2\Delta_o \pm eV_z$ . Both our Al and Be data show a well defined subgap peak whose magnitude grows dramatically as the parallel critical field is approached. Though this feature has previously been attributed to spin-orbit scattering, it is more consistent with fluctuations into a field induced mixed-spin state.

PACS numbers: 74.78.Db, 74.40.+k, 74.50.+r

With recent discoveries of itinerant ferromagnetic superconductors, represented by  $UGe_2$  [1] and  $ZrZn_2$  [2], and Fulde-Ferrell-Larkin-Ovchinnikov (FFLO) superconductivity in  $CeCoIn_5$  [3, 4], research on systems exhibiting a non-trivial interplay between magnetism and superconductivity has moved to the forefront on condensed matter physics. In this Letter we probe the spin states of superconducting Al and Be films in high parallel magnetic fields via spin polarized electron tunneling measurements [5]. The films are sufficiently thin so as to restrict the transverse motion of electrons, thus allowing us to access the high field regime while maintaining time reversal symmetry [6] up to the Clogston-Chandrasekhar critical field  $H_{c||} = \sqrt{2}\Delta_o/(g\mu_B)$ , where  $g$  is the Landé  $g$ -factor,  $\mu_B$  is the Bohr magneton, and  $\Delta_o$  is the superconducting gap [7]. Though the films are too disordered to support a FFLO phase [8], they are a model system for studying the spin states of BCS superconductivity in the presence of a non-negligible Zeeman field that ultimately drives the first-order spin-paramagnetic transition associated with  $H_{c||}$  [8, 9] and the long conjectured FFLO regime just above  $H_{c||}$  [8]. Tunneling measurements in fields  $H_{||} \gtrsim \frac{1}{2}H_{c||}$  reveal a subgap peak in the DOS spectrum, shifted down from the primary BCS peak by the Zeeman energy. The magnitude of the satellite peak varies as the square root of the reduced field. Though this peak has previously been attributed to spin-orbit (SO) scattering in Al [10], it is also manifest in the much lighter element Be, suggesting that it is a property of the high field condensate.

In the mid 1970's Tedrow, Meservey, and coworkers conducted a series of tunneling experiments on paramagnetically limited Al films. They showed that the tunneling spectrum of a superconductor-insulator-superconductor (S-I-S) junction, in which both the film and the counter-electrode are thin, will not exhibit a Zeeman splitting so long as there is no spin mixing or spin flip processes [8]. Assuming that the gap is  $\Delta_o$  on either side of the junction, then the tunneling spectrum has a single BCS peak at the usual  $|eV| = 2\Delta_o$ , independent of the Zeeman energy  $eV_z = g\mu_B H_{||}$ , where  $e$  is the electron charge. If, however, there is spin flip during the tunneling, then satellite peaks will appear at energies  $|eV| = 2\Delta_o \pm eV_z$  [8, 10]. Similarly, if there is a mechanism by which the spin eigenstates are partially mixed, then there will be a minority-spin satellite peak in the spectrum at  $|eV| = 2\Delta_o - eV_z$  [10]. No spin flip effects have ever been reported for tunneling through standard non-magnetic oxides such as  $Al_2O_3$ . However, spin mixing has been observed, the origin of which is the primary focus of this Letter.

Spin-orbit scattering is known to cause spin mixing and in thin films the SO scattering rate,  $1/\tau_{so}$ , increases with increasing atomic mass  $Z$  as  $\tau_s/\tau_{so} \sim Z^4$ , where  $\tau_s$  is the surface scattering time [11], suggesting that light elemental films are the best candidates for purely spin singlet superconductivity. Ironically, the first direct electron tunneling evidence of spin mixing was obtained in thin Al films using the S-I-S configuration described above [10]. A small subgap peak in the tunneling DOS was seen in 5 nm thick crossed Al films at the voltage  $|eV| = \Delta_{Film1} + \Delta_{Film2} - eV_z$ , consistent with a finite SO scattering rate. However, earlier measurements of the Knight shift in Al films showed that the shift extrapolated to zero at  $T=0$  in accord with BSC theory, suggesting that  $1/\tau_{so} \sim 0$  in Al [12]. More recent studies of the spin paramagnetic transition in Al and Be films have revealed both tricritical point behavior [13, 14] and quasi-coherent fluctuation modes [15] that are inconsistent with a finite SO scattering rate [8, 15].

The Al (Be) films used in these experiments were made by e-beam deposition of 3 - 5 nm of 99.999% Al (99.5% Be) onto fire polished glass microscope slides cooled to 84 K. Typical deposition rates were  $\sim 0.1$  nm/s in a vacuum of  $\sim 0.5$   $\mu$ Torr. The Al (Be) films had a transition temperature  $T_c \sim 2.7$  K ( $T_c \sim 0.5$  K) and a parallel critical field

$H_{c\parallel} \approx 6.0$  T ( $H_{c\parallel} \approx 1.0$  T). Tunnel junctions were formed by exposing the films to atmosphere for 0.2 – 1 hours in order to form a native oxide. Then an Al (Be) counter-electrode of the same thickness as the film was deposited directly on top of the film at 84 K. The integrity of the junctions was tested by measuring the dc I-V characteristics in zero magnetic field at T=50 mK. All of the tunneling data presented below are S-I-S. The films were aligned to within 0.1° of parallel by an *in situ* mechanical rotator.

In Fig. 1 we plot the zero field tunneling conductance as a function of bias voltage for a 2.7-nm Al film and a 4-nm Be film, each with a normal state sheet resistance  $R \sim 1$  kΩ. In order to compare the Al and Be spectra, we have normalized the bias voltage by each film’s respective gap. Within the resolution of the measurements, it is reasonable to assume that the superconducting gap of a film is the same as that of its counter-electrode  $\Delta_{Film} \sim \Delta_{CE} \sim \Delta_o$ , where  $\Delta_o$  is the zero temperature, zero field gap. At low temperatures the tunneling conductance is directly proportional to the quasiparticle density of states [17]. Note the very sharp BCS DOS peaks at  $2\Delta_o$  in Fig. 1. In Fig. 2 we show the spectra at several subcritical values of  $H_{\parallel}$ . The Al spectra are shown in a semi-log plot in order to better display the subgap features, and the Be curves have been shifted for clarity. Note that the position of the primary peak is relatively insensitive to field even at fields very near  $H_{c\parallel}$ , and that, as expected, it displays no Zeeman splitting. In contrast, there is a subgap feature whose magnitude and position are a function of field. The Al data in Fig. 2, displays the spin mixing feature first reported in Al by Meservey and Tedrow, though the peaks are somewhat sharper than those in Ref. 10 due to fact that the data were taken at 50 mK as opposed to 400 mK. Assuming that the surface scattering rates of the Al and Be films are comparable, then  $1/\tau_{so}$  of the Be film should be two orders of magnitude smaller than that of Al. Consequently, it seems unlikely that the supgap peaks in the Be data are due to SO scattering, which calls into question its role in the Al data. (The zero bias peaks in the Be spectra are a finite temperature effect, see Fig. 4 caption). Broken inversion symmetry can also produce a mixing of the spin singlet and triplet pairings in the presence of SO scattering [16]. However, this mechanism appears to require an intrinsic SO scattering rate that is inconsistent with the tricritical point behavior of the films.

The positions of the primary and subgap peaks, such as those in Fig. 2, are plotted in Fig. 3. For data close to the critical field, we were careful to insure that both the film and the counter-electrode were superconducting by monitoring the in-plane resistivity of each. We have normalized the voltage and field axes by the gap values in order to collapse the data sets. The weak quadratic field dependence of primary peak position, shown as solid symbols, is due to pair breaking [17]. The open symbols represent the position of the subgap features. Both the Al and Be data fall on the dashed line which represents the zero field gap minus the Zeeman energy assuming  $g=2$ . Indeed, there is sufficient resolution in the peak positions to rule out the possibility of a weak S-I-N component of the spectrum which would produce peaks at  $|eV| = \Delta_o \pm eV_z/2$ .

To gain a better understanding of the origin of the subgap peak, we studied its dependence on temperature and field orientation. By rotating slightly out of parallel orientation in a sub-critical field, we could test the effect of breaking time reversal symmetry. If the subgap peaks arise from a quasi-coherent fluctuation mode, then they will likely require this symmetry [15]. This is indeed the case as can be seen in the top panel of Fig. 4, where a misalignment of only 2° completely washes out the feature, though the position of the primary peaks remains unchanged. In the bottom panel of Fig. 4 we compare a Be spectrum at 50 mK and 200 mK. The central peak in the 200 mK curve is the well known S-I-S finite temperature peak which occurs at  $|\Delta_{Film} - \Delta_{CE}| \sim 0$  [17]. Note that the Zeeman subgap peak is somewhat attenuated at higher temperature, and is therefore not activated.

It is particularly evident that the magnitude of the subgap peaks in the spectra of Fig. 2 grows as one approaches the spin-paramagnetic transition. We have subtracted the field dependent background from the peaks to get a relative measure of the peak magnitudes. Figure 5 shows the subgap peak magnitude as a function of the square-root of the reduced field  $[1 - H_{\parallel}/H_{c\parallel}]^{-1/2}$ . Though this scaling form was chosen empirically, the linearity of the data strongly suggests critical behavior associated with a fluctuation mode which is being stabilized by the parallel field.

In conclusion we believe that the spin-mixing feature is an intrinsic property of spin-paramagnetically limited BCS superconductivity and that the ground state of the system is significantly altered near the critical field. It seems likely that the observed mixing has implications for FFLO physics to the extent that the films are believed to have a stable FFLO phase just above  $H_{c\parallel}$  in the zero scattering limit. Clearly, in the absence of disorder the system must find a way to evolve from spin singlet zero momentum pairing to the finite momentum depaired state of FFLO [18]. The nature of this process, particularly in the presence of disorder, remains an open question.

We gratefully acknowledge enlightening discussions with Robert Meservey, Kun Yang, Shivaji Sondhi, Igor Aleiner, Dana Browne, R.G. Goodrich, and David Young. This work was supported by the National Science Foundation under Grant DMR 02-04871.

---

[1] S. Saxena *et al.*, Nature **406**, 587 (2000).

[2] C. Pfleiderer *et al.*, Nature **412**, 58 (2001).

[3] P. Fulde and R.A. Ferrell, Phys. Rev. **135**, A550 (1964); A.I. Larkin and Y.N. Ovchinnikov, J. Exptl. Theoret. Phys. (USSR) **47**, 1136 (1964), [Sov. Phys. JETP **20**, 762, (1965)].

[4] A. Bianchi *et al.*, Phys. Rev. Lett. **89**, 137002 (2002); H.A. Radovan *et al.*, Nature **425**, 51 (2003).

[5] I. Giaever, Phys. Rev. Lett. **5**, 147 (1960).

[6] I.L. Aleiner and B.L. Altshuler, Phys. Rev. Lett. **79**, 4242 (1997).

[7] A.M. Clogston, Phys. Rev. Lett. **9**, 266 (1962); B.S. Chandrasekhar, Appl. Phys. Lett. **1**, 7 (1962).

[8] P. Fulde, Adv. Phys. **22**, 667 (1973).

[9] W. Wu and P.W. Adams, Phys. Rev. Lett. **73**, 1412 (1994).

[10] P.M. Tedrow and R. Meservey, Phys. Rev. Lett. **27**, 919 (1971). R. Meservey, P.M. Tedrow, and R.C. Bruno, Phys. Rev. B **11**, 4224 (1975).

[11] R. Meservey and P.M. Tedrow, Phys. Rev. Lett. **41**, 805 (1978).

[12] R.H. Hammond and G.M. Kelly, Phys. Rev. Lett. **18**, 156 (1966).

[13] V.Yu. Butko and P.W. Adams, Phys. Rev. Lett. **83**, 3725 (1999).

[14] P.W. Adams, P. Herron, and E.I. Meletis, Phys. Rev. B **58**, R2952 (1998).

[15] V. Yu. Butko, P.W. Adams, and I.L. Aleiner, Phys. Rev. Lett. **82**, 4284 (1999); P.W. Adams and V.Yu. Butko, Physica B **284**, 673 Part 1 (2000); Hae-Young Kee, I.L. Aleiner, and B.L. Altshuler, Phys. Rev. B **58**, 5757 (1998).

[16] L.P. Gorkov and E.I. Rashba, Phys. Rev. Lett **87**, 037004 (2001); S.K. Yip, Phys. Rev. B **65**, 144508 (2002).

[17] M. Tinkam, *Introduction to Superconductivity* (McGraw-Hill, New York, 1996).

[18] K. Yang and S.L. Sondhi, Phys. Rev. B **57**, 8566 (1998).

### Figures

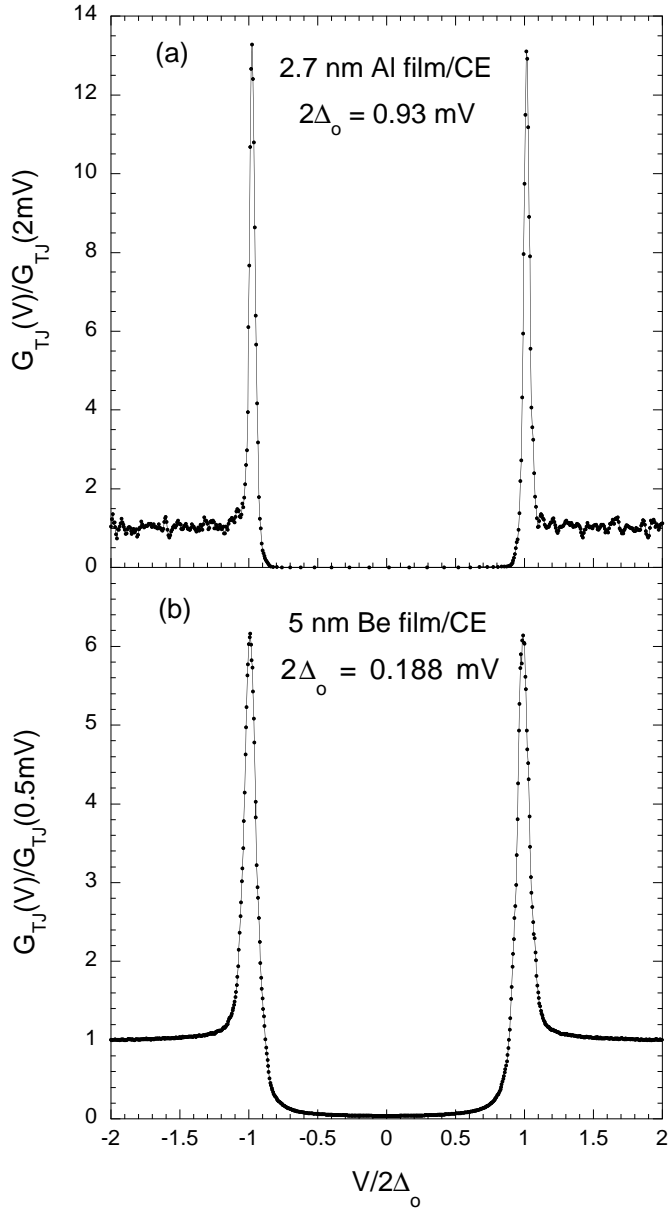


FIG. 1: S-I-S tunneling in zero field at  $T=50$  mK for an Al film (A) and Be film (B). The films and their respective counter-electrodes were identical. The tunnel junction conductances are plotted as a function of the bias voltage normalized by the sum of the zero field gaps  $2\Delta_o = \Delta_{Film} + \Delta_{CE}$ .

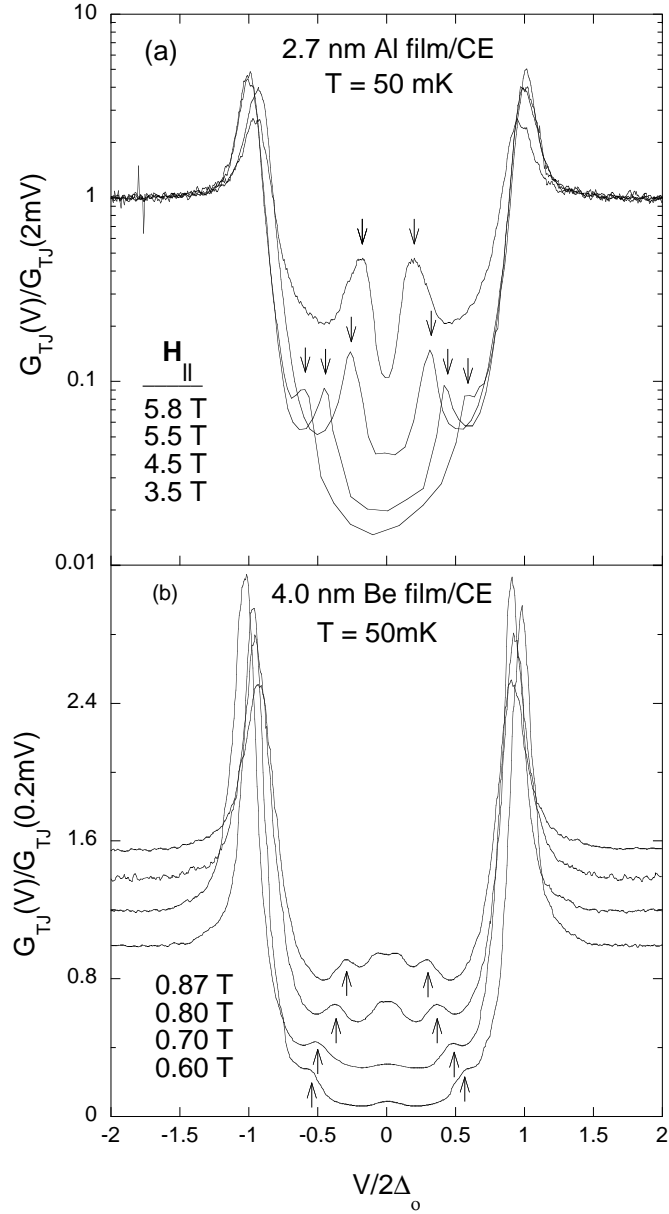


FIG. 2: Tunneling spectra of the films in Fig. 1 at several values of parallel magnetic field, where  $H_{c\parallel} = 5.9$  T for the Al film, and 0.9 T for the Be film. The arrows show the location of the subgap peaks. The Be curves have been shifted for clarity.

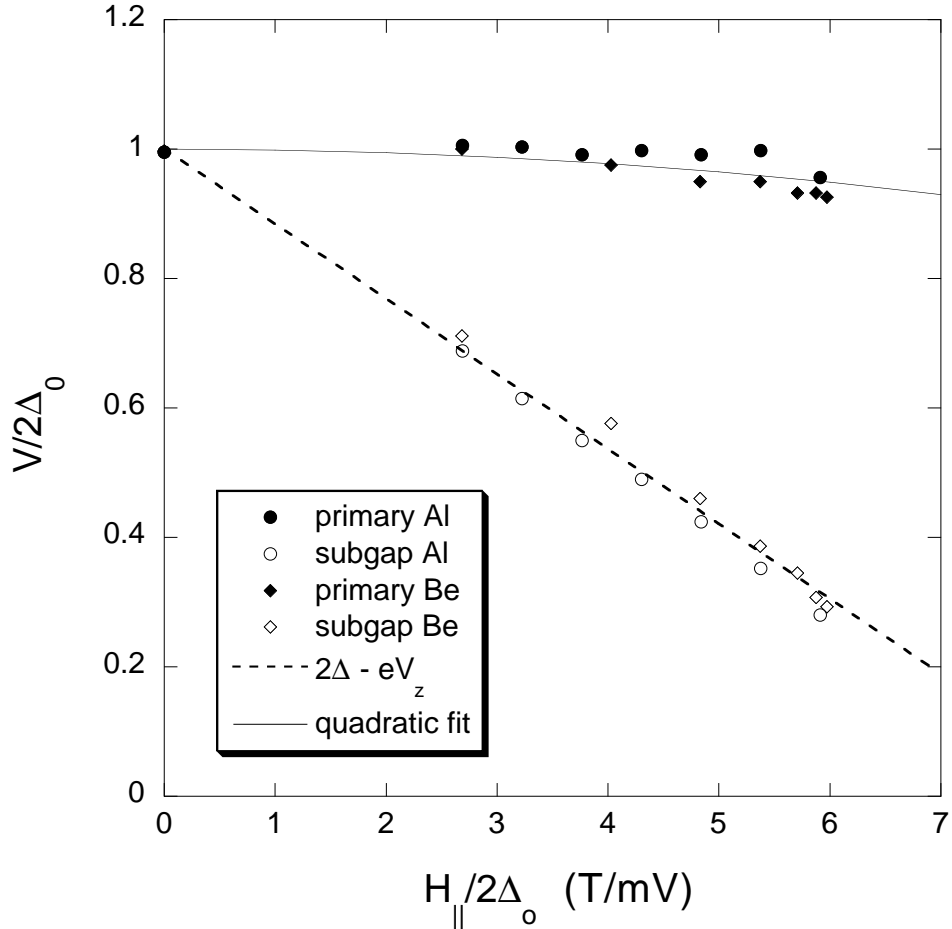


FIG. 3: Voltage positions of the primary and subgap peaks from spectra such as that in Fig. 2. The voltages and fields have been normalized by  $2\Delta_0$  in order to collapse the data sets. The dashed line represents  $2\Delta_0 - eV_z$ , where  $eV_z$  is the Zeeman energy.

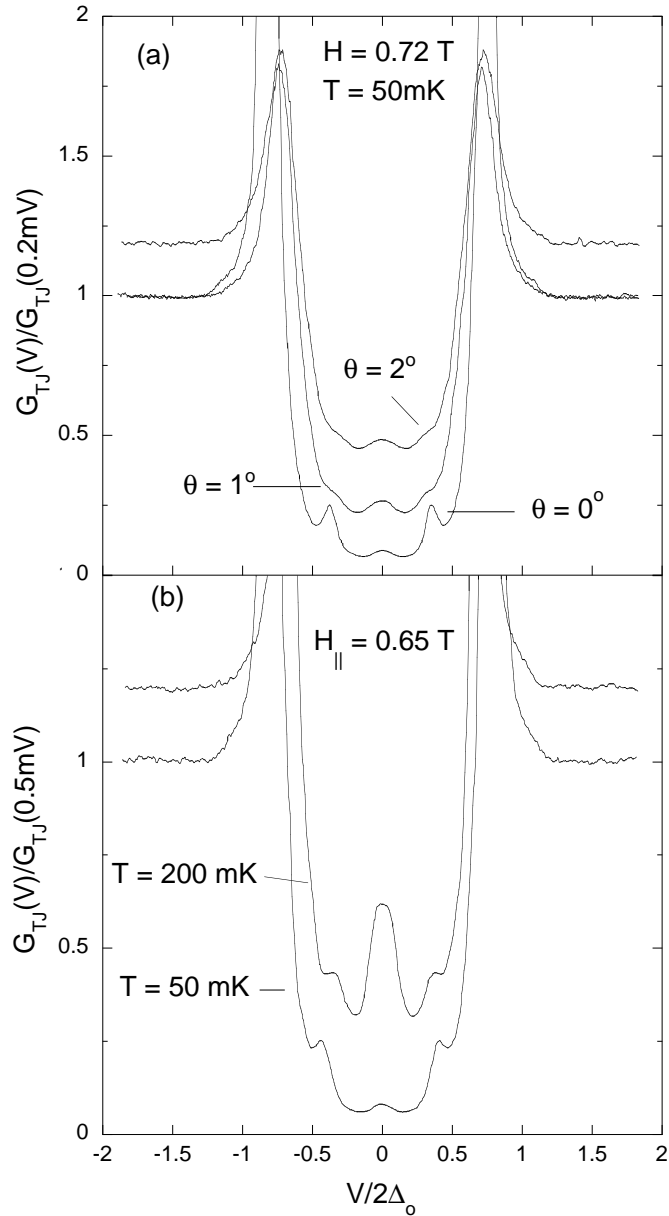


FIG. 4: (A) Effect of rotation out of parallel orientation on the tunneling spectra of a 4 nm Be film. Note the sensitivity of the subgap peak to  $\theta$ , where  $\theta = 0^\circ$  corresponds to parallel orientation. The  $\theta = 2^\circ$  curve has been shifted for clarity. (B) Tunneling spectra of the Be film at two different temperatures. The central peak in the 200 mK curve is the usual S-I-S finite temperature peak at  $|\Delta_{Film} - \Delta_{CE}| \sim 0$ .

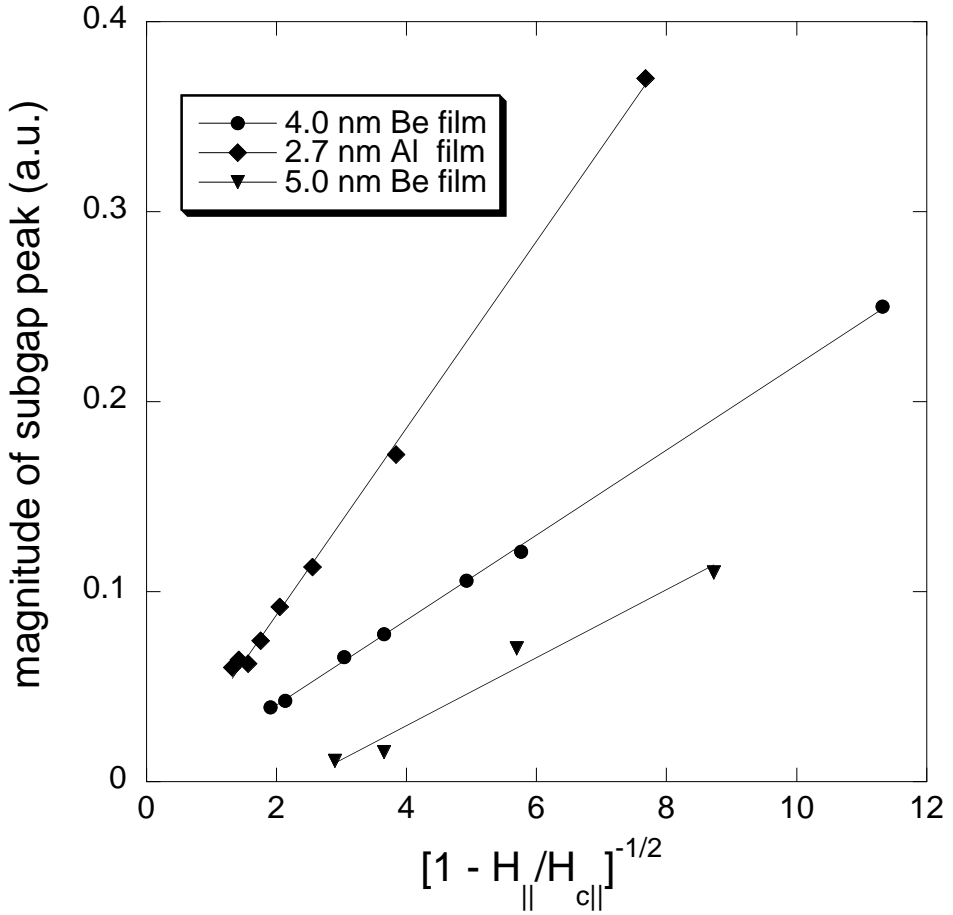


FIG. 5: Scaling behavior of the magnitude of the subgap peak near  $H_{c\parallel}$ . The low temperature normal state sheet resistance of the 4-nm Be film and the 2.7-nm Al film were  $\sim 1$  k $\Omega$ . The resistance of the 5-nm Be film was  $\sim 0.3$  k $\Omega$ . The parallel critical field values were  $H_{c\parallel} = 5.900$  T, 1.144 T, and 0.897 T for the Al film, 5-nm Be film, and the 4-nm Be film, respectively.